Electronic Properties of Thiolate Compounds of Oxomolybdenum(V) and Their Tungsten and Selenium Analogues. Effects of ^{17}O, ^{98}Mo, and ^{95}Mo Isotope Substitution upon ESR Spectra

Graeme R. Hanson, Andrew A. Brunette, Angus C. McDonell, Keith S. Murray,[1] and Anthony G. Wedd*

Contribution from the Department of Inorganic and Analytical Chemistry, La Trobe University, Bundoora, 3083, Australia, and the Department of Chemistry, Monash University, Clayton, 3168, Australia. *Received July 22, 1980*

Abstract: The series of crystalline, mononuclear $B^+[MO(XR)_4]^-$ and triply bridged binuclear $B^+[M_2O_2(XR)_6(OMe)]^-$ (M = Mo, W; X = S, Se; R = aryl; B = quaternary cation) salts have been isolated and the anions $[MoO(SR)_4]^-$ (R = Et, CH_2Ph) stabilized in solution at −60 °C. The mononuclear anions are intensely colored due to a ligand-to-metal charge-transfer transition which is absent in the binuclear species. The magnetic susceptibilities of $(Et_4N)[MO(SPh)_4]$ show a Curie dependence in the range 300–4.2 K with minor deviations in the tungsten compound. The behavior is essentially that of magnetically dilute $4d^1$ and $5d^1$ systems exhibiting a tetragonal ligand field and greatly reduced spin–orbit coupling on the metal. The presence of strong spin–spin coupling in the binuclear compounds leads to magnetic moments close to 0. ESR spectra (at X- and Q-band frequencies) of the mononuclear anions exhibit axial symmetry, and ^{98}Mo and ^{95}Mo isotope substitution and computer simulation permit accurate extraction of the g and hyperfine tensor anisotropies. Exceptionally narrow line widths permit observation of ^{17}O-superhyperfine coupling in ^{17}O-enriched $[^{98}MoO(SPh)_4]^-$ ($a = 2.2 \times 10^{-4}$ cm^{-1}).

In the context of the presence of both oxo and sulfur ligands bound to molybdenum in the molybdo–iron redox enzymes[2] sulfite oxidase and xanthine oxidase, we have recently synthesized and structurally characterized[3–6] three series of thiolate anions of oxomolybdenum(V): (i) mononuclear $[MoO(SR)_4]^-$ (I), (ii) triply bridged, binuclear $[Mo_2O_2(SR)_6Z]^-$, (e.g., II), and (iii) bis-μ-oxo, binuclear $[Mo_2O_4(SR)_4]^{2-}$ (III).

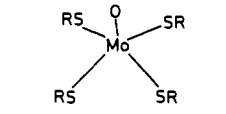

I

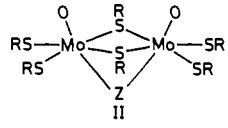

II

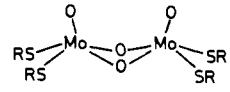

III

The paramagnetic anions I exhibit[3,5] a $^2B_2(b_2{}^*{}^1)$ ground state and, for R = aryl, are kinetically stable in solution. They convert[6] into the spin-coupled anions II when a ligand capable of occupying the unique bridging position Z is available; this prevents isolation of I (R = alkyl) at room temperature as $[Mo_2O_2(SR)_7]^-$ is formed.

The present paper demonstrates that $[MoO(SR)_4]^-$ (R = CH_2Ph, Et) can be stabilized at −60 °C, describes the synthesis of the $[MO(XR)_4]^-$ and $[M_2O_2(XR)_6(OMe)]^-$ (M = Mo, W; X = S, Se; R = aryl) series of anions, and presents a detailed comparison of their electronic spectral, ESR, and bulk magnetic susceptibility properties. In particular, isotope enrichment and computer simulation is employed for accurate estimation of the **g** and hyperfine (^{95}Mo, ^{183}W) tensor components from the ESR spectra of $[MO(XR)_4]^-$, and exceptionally narrow line widths permit observation of ^{17}O-superhyperfine coupling in ^{17}O-enriched $[^{98}MoO(SPh)_4]^-$.

* To whom correspondence should be addressed at La Trobe University.

Experimental Section

Synthesis. All manipulations were carried out under an atmosphere of purified dinitrogen or argon. Analytical reagent grade solvents were dried and distilled before use. Thiols RSH (R = Ph, *p*-tolyl, C_6Cl_5, $PhCH_2$, Et) were obtained commercially and dried over and fractionally distilled off molecular sieves. PhSeH was prepared by a literature method[7] under strictly anaerobic conditions in subdued light in an adequate fume hood and was sealed into glass ampules for storage. PhSeSePh was prepared by modification[8] of the above procedure.[7]

Pyridinium Pentachlorooxomolybdate(V), $(pyH)_2[MoOCl_5]$. A literature method[9] was refined to provide the high yields required for isotopic substitution. A solution of hydrazine hydrate (3.15 g, 63 mmol) in HCl (11.3 M, 180 cm^3) was added to $Na_2MoO_4{\cdot}2H_2O$ (8.2 g, 34 mmol) and heated to 80 °C for 3 h to produce a green solution over a white solid (NaCl). The mixture was refrigerated at −20 °C overnight and filtered while cold. Pyridine (9 cm^3, 112 mmol) was added dropwise to the filtrate at 50 °C and the system slowly cooled to −20 °C. The bright green needles were filtered, sucked free of mother liquor, and dried under vacuum; yield 9.2 g (65%).

Pyridinium Tetrabromooxomolybdate(V), $(pyH)[MoOBr_4]$. This synthesis combines literature[9,10] approaches to related compounds to produce a high-yield synthesis. A solution of $Na_2MoO_4{\cdot}2H_2O$ (4.1 g, 16.5 mmol) in HBr (9 M, 20 cm^3) was evaporated nearly to dryness at 130 °C. Another aliquot of acid was added, the evaporation repeated, a further aliquot added, and the mixture allowed to stand at −20 °C overnight. After the cold mixture was filtered, pyridine (2 cm^3, 25 mmol) was added to the filtrate at 40 °C to produce a red-orange crystalline

(1) Monash University.
(2) (a) Cramer, S. P.; Gray, H. B.; Rajagopalan, K. V. *J. Am. Chem. Soc.* **1979**, *101*, 2772–2774. (b) Tullius, T. D.; Kurtz, S. M.; Conradson, S. D.; Hodgson, K. O. *Ibid.* 2776–2779. (c) Bordas, J.; Bray, R. C.; Garner, C. D.; Gutteridge, S.; Hasnain, S. S. *J. Inorg. Biochem.* **1979**, *11*, 181–186.
(3) Boyd, I. W.; Dance, I. G.; Murray, K. S.; Wedd, A. G. *Aust. J. Chem.* **1978**, *31*, 279–284.
(4) Dance, I. G.; Wedd, A. G.; Boyd, I. W. *Aust. J. Chem.* **1978**, *31*, 519–526.
(5) Bradbury, J. R.; Mackay, M. F.; Wedd, A. G. *Aust. J. Chem.* **1978**, *31*, 2423–2430.
(6) Boyd, I. W.; Dance, I. G.; Landers, A. E.; Wedd, A. G. *Inorg. Chem.* **1979**, *18*, 1875–1885.
(7) Foster, D. G. *Org. Synth.* **1955**, *3*, 771–773.
(8) Sharpless, K. B.; Lauer, R. F. *J. Am. Chem. Soc.* **1973**, *95*, 2697–2699.
(9) Sasaki, Y.; Taylor, R. S.; Sykes, A. G. *J. Chem. Soc., Dalton Trans.* **1975**, 396–400.
(10) Saha, H. K.; Bannerjee, A. K. *Inorg. Synth.* **1974**, *15*, 100–103.

0002-7863/81/1503-1953$01.25/0

precipitate of (pyH)[$MoOBr_4$] which, upon cooling to −20 °C, turned yellow-brown due to coprecipitation of $(pyH)_2[MoOBr_5]$. After filtration, the product was sucked free of mother liquor and heated at 100 °C under vacuum to produce a sublimate of pyHBr and a residue of (pyH)[$MoOBr_4$]; yield 6.4 g (77%). Anal. ($C_5H_6Br_4MoNO$) C, H, N, Br.

Pyridinium Tetrachlorooxotungstate(V), (pyH)[$WOCl_4$]. This high-yield synthesis is based upon refinement of literature[11,14c] methods. Ammonium chloride (1.2 g, 22.4 mmol) was dissolved in concentrated HCl (33 cm^3) at 60 °C. The material formulated[11] as $(NH_4)_2WO_2(C_2O_4)_2$ (5 g, 11.2 mmol) was added slowly over 0.5 h. After being cooled in an ice–salt bath, the solution was saturated with HCl gas and stored overnight at −20 °C. The dark-green product $(NH_4)_2[WOCl_5]$ was filtered and dried under vacuum; yield 3.8 g (82%). A solution of $(NH_4)_2[WOCl_5]$ (2 g, 4.84 mmol) in concentrated HCl (48 cm^3) was stirred for 0.5 h and filtered, and the filtrate was heated to 40 °C. Pyridine (0.9 cm^3, 11.2 mmol) in concentrated HCl (8 cm^3) was added dropwise. The system was saturated with HCl gas at 0 °C and stored at 4 °C overnight. Brown crystals were filtered and dried under vacuum; yield 1.5 g (70%). Anal. ($C_5H_6Cl_4NOW$) C, H, Cl, N. Attempts to scale-up this synthesis were unsuccessful.

Thiolate Species. B[$MoO(SR)_4$] and B[$Mo_2O_2(SR)_6(OMe)$] (B = quaternary cation; R = Ph, *p*-tolyl, C_6Cl_5) were synthesized[3,6] with the use of $(pyH)_2[MoOCl_5]$ or (pyH)[$MoOBr_4$] as sources of molybdenum. Sufficient base was used to accommodate protons derived from both PhSH and PyH^+. Purple mononuclear and yellow binuclear tungsten salts were prepared analogously from (pyH)[$WOCl_4$], but with lower yields.

Selenolate Species. Tetraethylammonium Tetrakis(benzeneselenolato)oxomolybdate(V). (Et_4N)[$MoO(SePh)_4$]. A solution of PhSeH (1.24 g, 8 mmol) and Et_3N (1.64 cm^3, 12 mmol) was added dropwise to $(pyH)_2[MoOCl_5]$ (0.89 g, 2 mmol) in MeCN (10 cm^3) cooled in an ice bath. The intense-blue mixture was rapidly filtered, the volume reduced to about 5 cm^3, and Et_4NI (0.63 g, 2.5 mmol) in MeOH (15 cm^3) rapidly added to precipitate an oily green-blue solid. The mother liquor was immediately filtered off and the solid recrystallised from MeCN/MeOH to give a deep-blue crystalline solid.

Tetraethylammonium Tetrakis(benzeneselenolato)oxotungstate(V). A solution of PhSeH (1.4 g, 8.9 mmol) and Et_3N (1.6 cm^3, 11.2 mmol) in MeCN (10 cm^3) was added dropwise to (pyH)[$WOCl_4$] (0.94 g, 2.2 mmol) in MeCN (10 cm^3) cooled to −15 °C. The intense-blue mixture was rapidly filtered. The volume was reduced to about 5 cm^3 at −15 °C and Et_4NBr (1.15 g, 5.5 mmol) in *i*-PrOH (20 cm^3) rapidly added to precipitate dark blue crystals. The product was immediately filtered, washed with *i*-PrOH, and dried under vacuum.

Tetraethylammonium Hexakis(benzeneselenolato)methoxybis(oxomolybdate(V)), (Et_4N)[$Mo_2O_2(SePh)_6(OMe)$]. Sodium borohydride (0.15 g, 3.9 mmol) was carefully added via a side-arm addition flask to PhSeSePh (0.61 g, 2.0 mmol) in MeOH (15 cm^3). The solution was added dropwise to (pyH)[$MoOBr_4$] (0.5 g, 1.0 mmol) and Et_4NBr (0.3 g, 1.5 mmol) in MeOH (10 cm^3) to precipitate maroon crystals from a dark red solution. The product can be recrystallized at 60 °C from MeCN/MeOH.

The brown tungsten salt is similarly prepared from (pyH)[$WOCl_4$].

Isotopic Substitution. ^{95}Mo and ^{98}Mo (isotopic abundances 96.47 and 97.23 atom %, respectfully) were obtained as MoO_3 from Oak Ridge National Laboratory. ^{17}O (isotopic abundances 24.9 and 52.4 atom %) was obtained as H_2O from Norsk Hydro and Monsanto Research Corp., respectively.

Sodium molybdate was prepared from a finely ground mixture of MoO_3 and Na_2CO_3 by heating at 620 °C in a platinum crucible for 12 min. Thermogravimetric analysis confirmed stoichiometric loss of CO_2. Differential thermal analysis allowed observation of a phase change in Na_2MoO_4 at 640 °C and its known melting point at 683 °C. After being allowed to stand in air, the IR spectrum of the product was indistinguishable from that of a bona fide sample of $Na_2MoO_4 \cdot 2H_2O$.

Molybdate was converted to $(pyH)_2[MoOCl_5]$ and (pyH)[$MoOBr_4$] in carefully designed semimicro Schlenck apparatus which minimized the number of physical transfers of solution and allowed precipitation of product directly onto glass-filter frit. This permitted yields of 80–95% of the ^{95}Mo- and ^{98}Mo-substituted halo species. The synthesis was modified for ^{17}O-enriched $(pyH)_2[^{98}MoOCl_5]$ by the use of anhydrous $Na_2[^{98}MoO_4]$, crystalline hydrazine hydrochloride, and saturated hydrochloric acid produced from anhydrous HCl gas and the ^{17}O-enriched water. A condenser cooled to −10 °C minimized loss of solvent during the heating step.

Solutions of isotopically substituted $[MoO(XR)_4]^-$ (X = S, Se) were prepared from the halo species. Typically, a solution of Et_3N (1.40 cm^3) and HSPh (0.05 cm^3) in MeCN (50 cm^3) was generated and an aliquot (2.1 cm^3) added to $(pyH)_2[MoOCl_5]$ (1.91 mg) to produce a blue solution of concentration 2.0 mmol in Mo with molar ratios of Mo:S:Et_3N = 1:4.7:97. A lower relative concentration of base led to intermediate subsitution products (Table IV, vide infra). The solution was immediately filtered into a quartz ESR tube and the room-temperature spectrum recorded immediately. For XR = SCH_2Ph and SEt, the synthetic system was maintained at about −60 °C in a DMF slush bath and the sample rapidly cooled to 77 K.

Physical Measurements. Electronic spectra were obtained in matched quartz cells in Cary Model 18 and Varian Series 634 spectrophotometers. ESR spectra were obtained at X-band frequency on a Varian E-9 spectrometer with an E-101 bridge and at Q-band frequency on a Varian E-15 spectrometer with an E-110 bridge. Bulk magnetic susceptibility measurements were measured at room temperature with use of a Faraday balance constructed from a Newport 4-in. electromagnet fitted with appropriate pole pieces and a Cahn RG electrobalance. $Hg[Co(SCN)_4]$ was the calibrant. A modified Oxford Instruments Faraday balance with superconducting solenoid was employed for the low-temperature study. Measurements were made at fields of 10 and 40 kG and no field dependence was evident. A gradient field of 1000 Gcm^{-1} was employed and calibrated with a sample of pure nickel. The temperature was measured by thermocouples (calibrated relative to a GaAs diode) suspended in the sample position.

Analysis of ESR Spectra. Both liquid and frozen-solution ESR spectra were simulated with programmes developed by Dr. J. R. Pilbrow[12] and modified by G.R.H. For the present systems, where necessary, spectra were fitted to an axial $S = {}^1/_2$ spin Hamiltonian

$$K = \beta H \cdot \mathbf{g} \cdot S + hcS \cdot \mathbf{A} \cdot I$$

where the notation has its usual meaning. The derived **g** and **A** values have nominal errors of ±0.001 and $\pm 0.1 \times 10^{-4}$ cm^{-1}. The isotopes ^{98}Mo, ^{98}Mo, and ^{183}W have nuclear spin $I = 0$, $^5/_2$ and $^1/_2$, respectively.

Results and Discussion

Synthesis. Previous synthesis of mononuclear[3] and triply bridged binuclear[6] molybdenum–thiolate species used moisture-sensitive $[MoOCl_3(THF)_2]$ as the source of molybdenum. The pyrdinium salts of $[MoOCl_5]^{2-}$, $[MoOBr_4]^-$, and $[WOCl_4]^-$ are cheaper, more conveniently synthesized and much more stable than $[MOCl_3(THF)_2]$ (M = Mo,[3] W[13]) and were used in the present work. Sufficient base was added to take up protons derived from the cation. The formation of the species $[MO(XR)_4]^-$ (M = Mo, W; X = S, Se) can be represented by eq 1. The observation of

$$(pyH)_{n-3}[MOY_n] + 4HXR + (n+1)NEt_3 \xrightarrow{MeCN} [MO(XR)_4]^- + nY^- + (n+1)[HNEt_3]^+ + (n-3)py \quad (1)$$

(X = S, Se; M = Mo, Y = Br, $n = 4$; M = Mo, Y = Cl, $n = 5$; M = W, Y = Cl, $n = 4$)

intermediate substitution products by ESR (vide infra) indicates that an equilibrium exists when $[M] \approx 10^{-3}$ M. However, at higher [M], a combination of the relatively low solubilities of $[HNEt_3]Y$ in MeCN and B[$MO(XR)_4$] (B = quaternary cation) in alcohols allows isolation of good yields of the latter salts.

All the mononuclear species, particularly the selenolates, are thermodynamically unstable to conversion to the spin-coupled triply bridged binuclear species. For R = alkyl, the mononuclear species cannot be isolated at room temperature (eq 2) but are

$$2[MO(XR)_4]^- \rightarrow [M_2O_2(XR)_7]^- + XR^- \quad (2)$$

relatively stable at −60 °C (vide infra). For R = aryl, XR apparently[6] cannot occupy the unique bridging position Z in II, and so $[MO(XR)_4]^-$ is stable until a source of ligand (e.g., OR′, NR_2') which can occupy that position is made available (eq 3). The

$$2[MO(XR)_4]^- + HOR' \rightarrow [M_2O_2(XR)_6(OR')]^- + XR^- + HXR \quad (3)$$

selenolate species $[M_2O_2(SePh)_6(OMe)]^-$ are conveniently pre-

(11) Collenberg, O. *Z. Anorg. Allg. Chem.* **1918**, *102*, 247–276.

(12) Toy, A. D.; Chaston, S. H. H.; Pilbrow, J. R.; Smith, T. D. *Inorg. Chem.* **1971**, *10*, 2219–2225.

(13) Levason, W.; McAuliffe, C. A.; McCullough, F. P., Jr. *Inorg. Chem.* **1977**, *11*, 2911–2916.

Table I. Characterization Data

compd	yield, %	microanalysis[a]	IR data,[b] cm^{-1} ν(MO)	ν(CO)	μ_B[c]
$Et_4N[MoO(SPh)_4]$	80	C, H, N, O, S[d]	934		1.72
$Et_4N[MoO(S\text{-}p\text{-tolyl})_4]$	60	C, H, N, O, S	932		1.80
$Et_4N[Mo_2O_2(SPh)_6(OMe)]$	90	C, H, N, O, S	936	1048	0.32
$Et_4N[Mo_2O_2(SCH_2Ph)_7]$	60	C, H, N, O, S	908		0.38
$Et_4N[MoO(SePh)_4]$	40	C,[e] H, N, Se	930		1.75
$Et_4N[Mo_2O_2(SePh)_6(OMe)]$	70	C, H, N, O, Se	932	1040	<0.3
$Ph_4As[Mo_2O_2(SePh)_6(OMe)]$	70	C, H, O, Se	939, 930	1045	<0.3
$Et_4N[WO(SPh)_4]$	50	C, H, N, O, S	943		1.34
$Ph_4As[WO(SPh)_4]$	45	C, H, O, S	949		
$Et_4N[WO(S\text{-}p\text{-tolyl})_4]$	45	C, H, N, O, S	939		1.32
$Et_4N[W_2O_2(SPh)_6(OMe)]$	28	C, H, N, O, S	944	1042	diamag[g]
$Et_4N[W_2O_2(S\text{-}p\text{-tolyl})_6(OMe)]$	26	C, H, N, O, S	944	1044	diamag
$Et_4N[WO(SePh)_4]$	40	C,[f] H, N, O, Se	943		1.30
$Et_4N[W_2O_2(SePh)_6(OMe)]$	20	C, H, N, O, Se	940	1055	

[a] All microanalyses agree with calculated values within ±0.4% except where indicated. [b] Nujol mulls. [c] Magnetic moment per mole of M, in solid state at room temperature. [d] Anal. Calcd for ($C_{32}H_{40}MoNOS_4$): S, 18.91. Found: S, 18.38. [e] Anal. Calcd for ($C_{32}H_{40}MoNOSe_4$): C, 44.36. Found: C, 43.12. [f] Anal. Calcd for ($C_{32}H_{40}NOSe_4W$): C, 40.27. Found: C, 39.66. [g] diamag = diamagnetic.

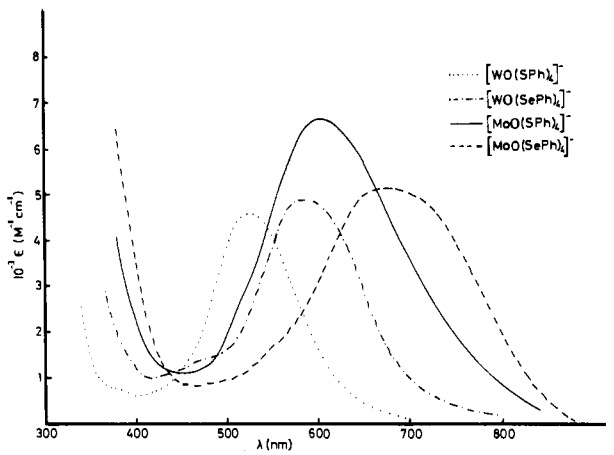

Figure 1. Electronic spectra of $Et_4N[MO(XPh)_4]$ in MeCN solution.

pared from selenolate (derived by borohydride reduction of diselenide) in methanol. Table I lists yield and characterization data for selected crystalline compounds isolated in substance.

Electronic Spectra. A most distinctive feature of the mononuclear compounds $[MO(XR)_4]^-$ is their intense colors due to optical transitions at 500–700 nm (Table II and Figure 1). Several points suggest these characteristic absorptions are ligand-to-metal charge transfer in origin.

(i) The magnitude of the extinction coefficients and the dependence of the absorption maxima on the nature of the ligand precludes assignment of the absorptions to the weak, essentially ligand-independent transitions in the 400–710-nm region which normally characterize[14] mononuclear oxo complexes of Mo(V) and W(V). These latter transitions may account for weak features seen in this region for several of the anions.

(ii) For the thiolate species $[MO(SR)_4]^-$, the displacement of the band energy to lower energy as the thiolate becomes more electron donating (R = C_6Cl_5 → Ph → *p*-tolyl) is expected for ligand-to-metal charge transfer.[15]

(iii) The substitution of Se for S or of Mo for W also displaces the band to lower energy (see Figure 2) and the trend is in qualitative agreement with Jørgensen's theory of charge-transfer spectra.[16] This approach utilizes optical electronegativities χ_{opt}

Table II. Electronic Spectra of Et_4N^+ Salts in MeCN

anion	abs max, nm	ext coeff,[a] M^{-1} cm^{-1}
$[MoO(SPh)_4]^-$	598	6 600
	324 sh, 287 sh	
	239	50 000
$[MoO(S\text{-}p\text{-tolyl})_4]^-$	610	7 100
	360 sh, 327 sh, 287 sh	
	240	58 000
$[MoO(SC_6Cl_5)_4]^-$	585	7 300
	342 sh, 280 sh	
	220	48 000
$[MoO(SePh)_4]^-$	675	5 100
	565 sh, 503 sh	
	340 sh	11 000
$[WO(SPh)_4]^-$	525	4 560
	380 sh, 230 sh	
	220	43 000
$[WO(S\text{-}p\text{-tolyl})_4]^-$	544	5 820
	390 sh	
	223	48 000
$[WO(SePh)_4]^-$	588	4 860
	465 sh	1 300
$[Mo_2O_2(SPh)_6(OMe)]^-$	505 sh	
	360 sh	17 400
	318 sh	
	258 sh	61 500
$[Mo_2O_2(SePh)_6(OMe)]^-$	507 sh, 415 sh	
	371 sh	15 200
$[W_2O_2(SPh)_6(OMe)]^-$	415 sh	7 500
	319 sh	18 800
$[W_2O_2(SePh)_6(OMe)]^-$	424 sh	
	365 sh	18 000

[a] Extinction coefficient.

to predict that energy *differences* of the first allowed band should be given by

$$\Delta E_{CT}\ (cm^{-1}) = 30000|\chi_{opt}(S) - \chi_{opt}(Se)|$$

for the *same* metal and by

$$\Delta E_{CT}\ (cm^{-1}) = 30000|\chi_{opt}(W^V) - \chi_{opt}(Mo^V)|$$

for the *same* ligand. Calculation of the difference terms from the data in Table II gives

$|\chi_{opt}(S) - \chi_{opt}(Se)| =$
0.065 ± 0.003 and $|\chi_{opt}(W^V) - \chi_{opt}(Mo^V)| = 0.075 \pm 0.003$

Estimates from other systems based upon terminally ligated S

(14) (a) Garner, C. D.; Hillier, I. H.; Kendrick, J.; Mabbs, F. E. *Nature (London)* **1975**, *258*, 138–139. (b) Garner, C. D.; Hill, L.; Howlader, N. C.; Hyde, M. R.; Mabbs, F. E.; Routledge, V. I. *J. Less-Common Met.* **1977**, *54*, 27–34. (c) Allen, E. A.; Brisdon, B. J.; Edwards, D. A.; Fowles, G. W. A.; Williams, R. G. *J. Chem. Soc.* **1963**, 4649–4657. (d) McAuliffe, C. A.; McCullough, P.; Werfalli, A. *Inorg. Chim. Acta* **1978**, *29*, 57–61.

(15) Lever, A. B. P. "Inorganic Electronic Spectroscopy"; Elsevier: Amsterdam, 1968; pp 224–248.

(16) Jørgensen, C. K. *Prog. Inorg. Chem.* **1970**, *12*, 101–158.

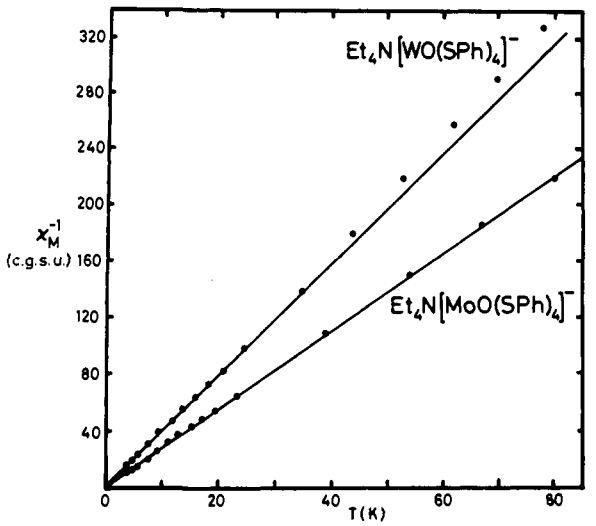

Figure 2. Reciprocal molar susceptibility vs. temperature plots for $Et_4N[MO(SPh)_4]$ (M = Mo, W). The solid lines do not represent calculated points but are best straight lines drawn through the lower temperature points.

and Se[17] and Mo^V and W^V hexahalide[16] and oxo[18] species also suggest values <0.1.

The absence of these intense absorptions in the spin-paired binuclear analogues $[M_2O_2(XR)_6(OMe)]^-$ (Table II)[6] suggests that the singly occupied HOMO $b_2^*(d_{xy}, Mo–X(\pi^*))$ is the metal-based orbital involved.[19] The only such ligand-to-metal transitions which are electric dipole allowed in C_{4v} symmetry are

$$^2B_2 \rightarrow {}^2B_2: \; b_2(M–X(\pi)) \rightarrow b_2^*(M–X(\pi^*))$$

$$^2B_2 \rightarrow {}^2E: \; e(M–O(\pi)) \rightarrow b_2^*(M–X(\pi^*))$$

Attempts to synthesize a suitable host lattice are underway as polarized crystal data would distinguish between these assignments.

Absorptions of comparable energy and intensity are observed[20] in reduced sulfite oxidase and xanthine oxidase and have been assigned to the molybdenum chromophore. Additionally, similar absorptions are seen in aqueous solutions of $[Mo_2O_4(cysteinate)_2]^{2-}$ where equilibria including mononuclear Mo(V)–cysteinyl species are proposed.[21]

Magnetic Susceptibility. The room-temperature magnetic moments given in Table I clearly show that the compounds can be divided into two classes. The binuclear species display very small positive susceptibilities in the case[6] of Mo(V) and diamagnetic susceptibilities in the case of W(V). These results are compatible with strongly antiferromagnetically coupled M(V) centers. The smaller value of μ_{eff} observed in the tungsten compounds more likely[22] reflects the larger spin–orbit coupling constant than a stronger exchange coupling constant.

The magnetic moments of the mononuclear complexes are within the ranges normally observed for such d^1 compounds of MoO^{3+} (1.7–1.8 μ_B) and WO^{3+} (1.3–1.5 μ_B). The smaller values for tungsten again reflect the presence of a larger spin–orbit coupling, although the spin–orbit coupling parameters in each case are considerably reduced from their free-ion values.[22,23] We have previously shown[3] that the $[MoO(SR)_4]^-$ complexes display Curie–Weiss behavior within the temperature range 300–90 K. This is expected for a $^2T_{2g}$ term which has been split by a combination of spin–orbit coupling and a strong tetragonal (C_{4v}) ligand field to yield a $^2B_2$ ground state. In the present study the temperature range has been extended to 4.2 K for the representative compounds $Et_4N[MO(SPh)_4]$. This was done partly to compare Mo^V with W^V but also to see if any nonlinear χ^{-1} vs. T behavior could be observed at low temperatures due to interactions between metal centers in the solid lattice. The reciprocal susceptibilities in the temperature range 80–4.2 K are plotted in Figure 2 and the data over the whole temperature range tabulated in Table III. The behavior is linear and Curielike in the molybdenum complex with an effective magnetic moment of 1.70 μ_B. Similar behavior is observed for the tungsten complex, although there appears to be a small divergance from the linear portion below ca. 40 K into another linear region above this temperature which has slightly higher slope. A concomitant small increase in μ_{eff} therefore occurs as the temperature decreases, i.e., 1.38 μ_B at 78.5 K and 1.42 μ_B at 4.3 K. This may, in part, be a result of the very small forces being measured at higher temperatures, but it is notable that such effects have been detected in previous studies of oxotetrahalogenomolybdenum(V) species.[22] There are a number of possible reasons which could explain these subtle effects such as temperature-dependent crystal lattice distortions, metal–ligand

Table III. Molar Susceptibilities[a]

$(Et_4N)[MoO(SPh)_4]$			$(Et_4N)[WO(SPh)_4]$		
T, K	χ_{Mo}[b]	μ_{eff}, μ_B	T, K	χ_W[b]	μ_{eff}, μ_B
4.3	82618	1.69	4.3	58004	1.42
5.0	72296	1.70	4.9	51169	1.42
6.1	59590	1.71	6.0	42287	1.43
7.7	46861	1.70	7.7	32520	1.42
9.3	38091	1.69	9.6	25640	1.41
11.1	31772	1.68	11.7	21086	1.41
13.1	27004	1.68	13.8	17960	1.41
15.2	23541	1.69	16.0	15555	1.41
17.4	20662	1.69	18.3	13749	1.42
19.6	18355	1.70	20.8	11979	1.41
23.4	15440	1.70	24.5	10146	1.41
38.9	9191	1.69	34.7	7180	1.41
53.9	6654	1.69	43.7	5556	1.39
67.4	5372	1.70	52.6	4591	1.39
80.2	4556	1.71	62.0	3828	1.39
91.8	3992	1.71	70.1	3422	1.39
103.4	3575	1.72	78.5	3052	1.38
114.4	3247	1.72	86.2	2768	1.38
118.5	3125	1.72	91.9	2594	1.38
142.9	2564	1.72	94.8	2539	1.39
169.1	2192	1.72	126.9	1896	1.39
193.4	1919	1.72	155.8	1523	1.38
218.2	1694	1.72	182.4	1282	1.37
240.1	1538	1.72	210.1	1103	1.36
262.4	1412	1.72	234.1	978	1.35
284.1	1311	1.72	258.3	877	1.35
			282.0	799	1.34
			300.7	752	1.34

[a] Units of χ are $10^6 \times cm^3\ mol^{-1}$. [b] Ligand correction is −333.

Table IV. Room-Temperature ESR Spectra of $[MoOCl_5]^{2-}$/HSPh/NEt_3 Solutions[a] in MeCN

proposed species[b]	g	10^4a, cm^{-1}
$[MoOCl_4(MeCN)]^-$	1.948	45
$[MoOCl_3(SPh)]^-$	1.966	c
$[MoOCl_2(SPh)_2]^-$	1.977	39
$[MoOCl(SPh)_3]^-$	1.983	37
$[MoO(SPh)_4]^-$	1.990	31

[a] 2×10^{-3} M in Mo; 9×10^{-5} M in S; $(0–200) \times 10^{-3}$ M in NEt_3. [b] See text. The substitution products may be 6-coordinate if MeCN formally enters the coordination sphere (see ref 24). [c] Not observed because of apparent overlap with other absorptions.

(17) Bobrik, M. A.; Laskowski, E. J.; Johnson, R. W.; Gillum, W. O.; Berg, J. M.; Hodgson, K. O.; Holm, R. H. *Inorg. Chem.* **1978**, *17*, 1402–1410.
(18) So, H.; Pope, M. T. *Inorg. Chem.* **1972**, *11*, 1441–1443.
(19) Suitable molecular orbitals models for the current compounds are described in Garner, C. D.; Hill, L. H.; Mabbs, F. E.; McFadden, D. L.; McPhail, A. T. *J. Chem. Soc., Dalton Trans.* **1977**, 853–858 and references therein.
(20) (a) Johnson, J. L.; Rajagopalan, K. V. *J. Biol. Chem.* **1977**, *252*, 2017–2025. (b) Garbett, K.; Gillard, R. D.; Knowles, P. F.; Stangroom, J. E. *Nature (London)* **1967**, *215*, 824–828.
(21) See ref 25, 95–99, for a summary of the present status of this complex system.
(22) Brisdon, D. J.; Edwards, D. A.; Machin, D. J.; Murray, K. S.; Walton, R. A. *J. Chem. Soc. A* **1967**, *1825*–1831.
(23) Hare, C. R.; Bernal, I.; Gray, H. B. *Inorg. Chem.* **1962**, *1*, 831–835.

Table V. ESR Parameters for Mononuclear Complexes[a]

anion	g	10^4a, cm^{-1}	$g_{\parallel}$	$g_{\perp}$	$10^4A_{\parallel}$, cm^{-1}	$10^4A_{\perp}$, cm^{-1}
$[MoO(SPh)_4]^-$	1.990[b]	32.3[c]	2.017[b]	1.979[b]	52.3[c]	22.3[c]
$[MoO(S\text{-}p\text{-}tolyl)_4]^-$	1.989	32.5	2.016	1.977	52.8	23.2
$[MoO(SCH_2Ph)_4]^-$	1.990[d]	32.3[d]	2.021	1.975	52.8	21.7
$[MoO(SEt)_4]^-$	1.986[d]	31.0[d]	2.018	1.972	52.9	22.2
$[MoO(SePh)_4]^-$	2.024[b]	30.0[c]	2.072[b]	2.005[b]	48.3[c]	21.2[c]
$[WO(SPh)_4]^-$	1.936	55.1[e]	2.018	1.903	78.1	44.4[e]
$[WO(S\text{-}p\text{-}tolyl)_4]^-$	1.935	55.1[e]	2.014	1.903	78.0	44.4[e]
$[WO(SePh)_4]^-$	1.971	50.6[e]	2.086	1.923	74.0	43.3[e]
$[MoOCl_4]^-$[f]	1.956	52.5	1.967	1.950	79.0	39.0

[a] 10^{-3} M in MeCN at room temperature and in 4:1 MeCN:DMF glasses at about 77 K. [b] Derived from ^{98}Mo-enriched samples. [c] Calculated to second order from ^{95}Mo-enriched samples. [d] In DMF at about −60 °C. [e] Derived via computer simulation. [f] Reference 19.

covalent bonding, or weak magnetic interactions. It is apparent, however, that these thiolato complexes of molybdenum and tungsten are essentially simple $S = {}^1/_2$ paramagnets with any intrinsic spin interactions being extremely weak.

Electron Spin Resonance. Typical Mo(V) and W(V) spectra in liquid solution include a central absorption due to resonance of molecules with even metal isotopes ($I = 0$). This is flanked by hyperfine lines due to resonance of molecules with odd metal isotopes ($I \neq 0$). There are six hyperfine lines due to ^{95,97}Mo (25.15 atom %; $I = {}^5/_2$) for molybdenum and two hyperfine lines due to ^{183}W (14.40 atom %; $I = {}^1/_2$) for tungsten. Isotope enrichment assists interpretation and accurate parameter extraction, especially in frozen-glass or single-crystal environments where overlap of the various components of the anisotropic branches of the spectra can occur.

The room-temperature spectrum of a 2×10^{-3} M solution of $(pyH)_2[MoOCl_5]$ in MeCN shows the presence of a single species ($g = 1.948$; Table IV). $[MoOCl_5]^{2-}$ readily[20] dissociates the axial Cl ligand, especially in coordinating solvents such as MeCN. Comparison of known[24] g values of $[MoOCl_5]^{2-}$ (1.940), $[MoOCl_4]^-$ (1.956), $[MoOCl_3(MeCN)_2]$ (1.944), and $[MoOCl_4(DMF)]^-$ (1.947) suggests the presence of $[MoOCl_4(MeCN)]^-$ in the present work. Addition of 4–5 mol equiv of HSPh followed by an increasing concentration of the base NEt_3 allows observation of an equilibrium involving a total of five species (Table IV). When 100 equiv of NEt_3 are present, the spectrum is indistinguishable from that[3] of a 2×10^{-3} M solution of $Et_4N[MoO(SPh)_4]$ ($g = 1.990$). The three species of intermediate g value are assigned as mono-, bi- and tri-benzenethiolate substitution products of $[MoOCl_4(MeCN)]^-$ on the basis of: (i) the smooth increase in g value and decrease in average hyperfine coupling constant a, and (ii) the increasing relative concentrations of the species with higher g values as the concentration of base increases. If these assignments can be accepted, this series provides some systematic data on the way in which g and a parameters vary with the number of thiolate ligands at a $[MoO]^{3+}$ center. It is interesting that the g and a ranges correlate well with the observed enzyme parameters.[25] However, it must be emphasized that closer comparison[25-27] of enzyme parameters with those of well-characterized model $[MoO]^{3+}$ compounds (including those reported in this paper) show significant differences in detail, especially in terms of the anisotropy of the **g** and **A** tensors.

Derived **g** and **A** tensor components are listed in Table V. Equivalent results were obtained at X- and Q-band frequencies. For $[MoO(SPh)_4]^-$, the **g** and **A** components were determined from ^{98}Mo ($I = 0$) and ^{95}Mo ($I = {}^5/_2$) enriched samples, respectively, (Figure 3a,b) and axial symmetry is confirmed. The assumption of coincidence of the **g** and **A** tensor coordinate axes leads to satisfactory computer simulation (e.g., Figure 3c) and is consistent with the observed[5] square pyramidal (C_{4v}) arrangement of ligand sulfur atoms around the central molybdenum atom in $Ph_4As[MoO(SPh)_4]$. The same assumption was made to estimate $A_{\perp}$ in the naturally-abundant tungsten species via computer simulation as only the parallel hyperfine lines are completely resolved (Figure 4).

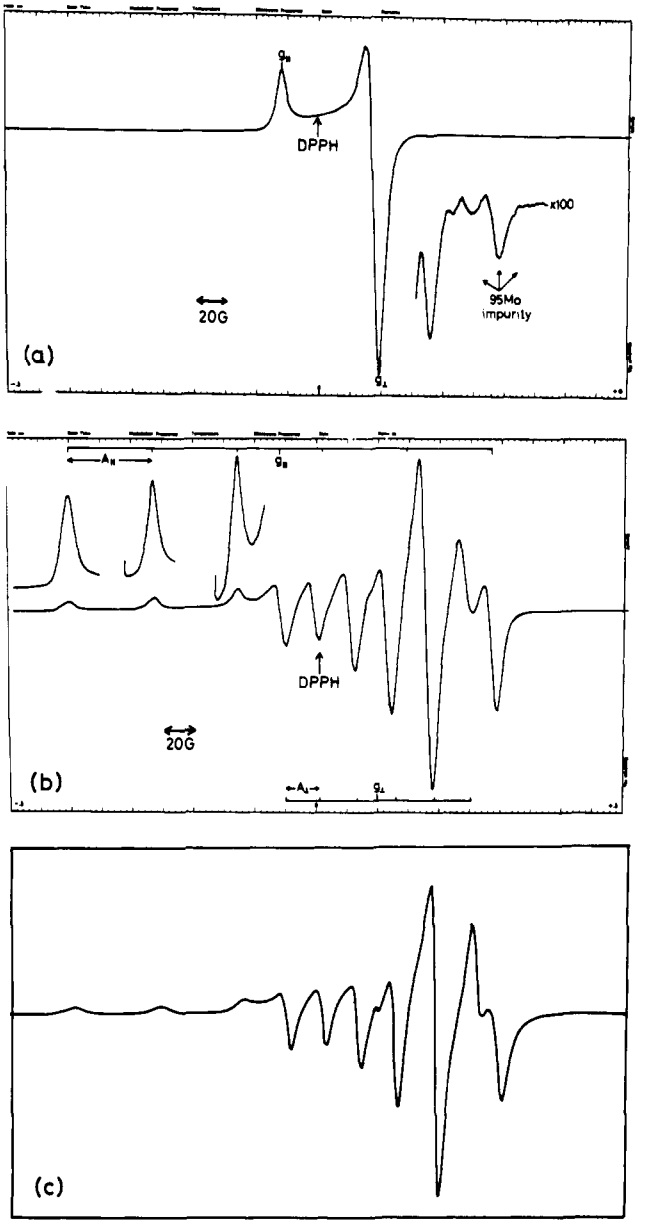

Figure 3. X-band ESR spectrum of 10^{-3} M $[MoO(SPh)_4]^-$ in 4:1 MeCN:DMF glass at 100 K: (a) 97.23 atom % ^{98}Mo; (b) 96.47 atom % ^{95}Mo; (c) computer simulation of (b).

While mononuclear species cannot be isolated at room temperature for R = CH_2Ph and Et, purple species can be stabilized

(24) (a) Garner, C. D.; Hyde, M. R.; Mabbs, F. E. *Inorg. Chem.* **1976**, *15*, 2327–2328. (b) Garner, C. D.; Hill, L. H.; Mabbs, F. E.; McFadden, D. L.; McPhail, A. T. *J. Chem. Soc., Dalton Trans.*, **1975**, 1299–1306.
(25) Stiefel, E. I. *Prog. Inorg. Chem.* **1976**, *22*, 1–223.
(26) Pariyadeth, N.; Newton, W. E.; Stiefel, E. I. *J. Am. Chem. Soc.* **1976**, *98*, 5388–5389.
(27) Scullane, M. I.; Taylor, R. D.; Minelli, M.; Spence, J. T.; Yamanouchi, K.; Enemark, J. H.; Chasteen, N. D. *Inorg. Chem.* **1979**, *18*, 3213–3219.

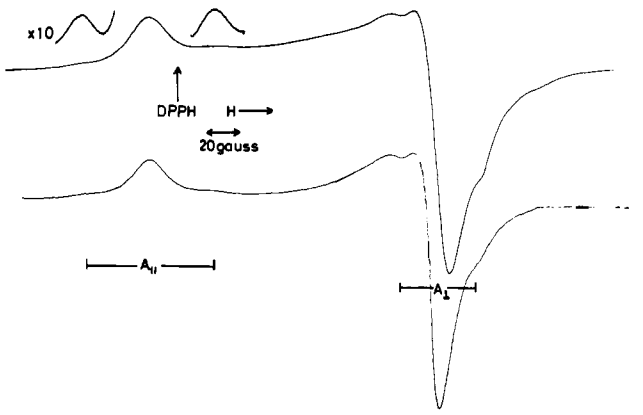

Figure 4. (a) X-band ESR spectrum of 10^{-3} M $[WO(SPh)_4]^-$ in a 4:1 MeCN:DMF glass at 77 K. (b) computer simulation of (a).

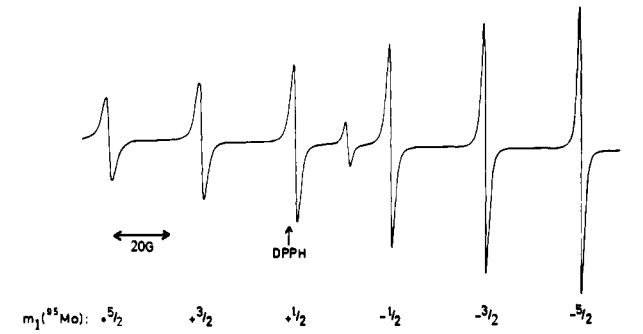

Figure 5. X-band ESR spectrum of 1.43×10^{-3} M $[^{95}MoO(SPh)_4]^-$ in MeCN at room temperature (96.47 atom % ^{95}Mo, 0.46 atom % ^{97}Mo; the central absorption is due to resonance on those molecules (3.12 atom %) containing even ($I = 0$) isotopes of Mo).

in solution with Mo:HSR:NEt_3 = 1:4:100 at −60 °C. ESR spectra indicate the presence of a single species, and those spectra and the color are attributed to the $[MoO(SR)_4]^-$ anion. The derived ESR (and electrochemical[28]) parameters indicate that the electronic state of molybdenum is essentially unaffected by the substitution of alkane- for benzenethiolate ligands. The electronic similarity of simple alkanethiolate and the cysteinate ligands has been emphasized[29] recently.

The $g_\parallel$ components of all the $[MO(XR)_4]^-$ anions easily exceed the free-electron value of 2.0023. Selenium spin–orbit coupling may contribute[30] significantly to the very high $g_\parallel$ values of the selenolate species. The availability of four anions $[MO(XPh)_4]^-$ provides a good opportunity for comparative single-crystal ESR studies, and such experiments are in progress.

The X-band solution spectrum of $[^{95}MoO(SPh)_4]^-$ at 300 K in MeCN is shown in Figure 5. It can be seen that the exceptionally narrow line widths (Table VI) of the hyperfine components vary with the nuclear spin orientation, m_I. Examination[31] of the

Table VI. Line Width and Anisotropy Data

compd	ΔH,[a] G	$\lvert g_\parallel - g_\perp \rvert$	$10^4 \cdot \lvert A_\parallel - A_\perp \rvert$, cm^{-1}
$[MoO(SPh)_4]^-$	1.71–2.95	0.038	30.0
$[MoO(SePh)_4]^-$	2.99–5.94	0.067	27.1
$[WO(SPh)_4]^-$	6.4[b]	0.115	33.8
$[WO(SePh)_4]^-$	8.1[b]	0.163	33.4
$[MoOCl_4(MeCN)]^-$	13.0–14.9	0.037	43.4
$[MoO(acac)_2Cl]$	9.5–10.3	0.018[c]	42.8[c]
$[VO(acac)_2]$[d]	7.35–14.41	0.039	109.0
$[Cu(acac)_2]$[d]	24.36	0.236	150.6

[a] The observed range of peak-to-peak line widths, ΔH, in the derivative spectra at 300 K for the observed hyperfine lines. [b] Estimated by computer simulation. [c] Reference 27. [d] Reference 32b.

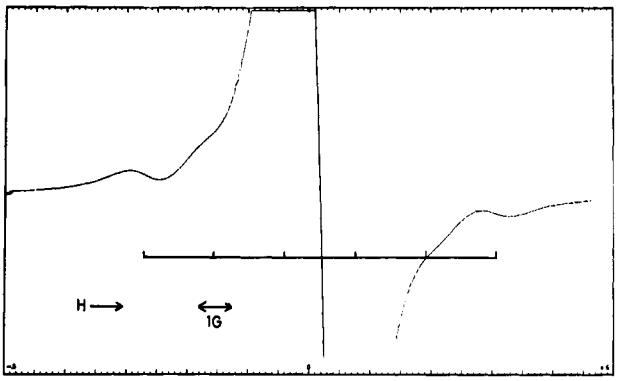

Figure 6. X-band ESR spectrum of 2×10^{-3} M $[^{98}MoO(SPh)_4]$ enriched with ^{17}O ($I = 5/2$; 24.9 atom %) in MeCN at room temperature.

variation of the peak-to-peak line widths, ΔH, of $[^{95}MoO(XPh)_4]^-$ (X = S, Se) in MeCN with temperature and field (X- and Q-band frequencies) show that (i) they obey the relationship[32]

$$\Delta H = \alpha' + \alpha'' + \beta m_I + \gamma m_I^2$$

(ii) α', β, and γ are proportional to η/T where η is the viscosity of MeCN at temperature T, and (iii) α'' varies linearly with T/η.

This confirms[32] that the major spin-relaxation mechanisms are due to anisotropy in the **g** and **A** tensors associated with the tumbling molecule in solution and that there is a residual line width α'' at least partially associated with a spin-rotational mechanism. The line widths for $[MoO(SPh)_4]^-$ at Q-band frequency can be qualitatively predicted[31] from those observed at X-band frequency.

Table VI, and related data, indicates that (i) the narrow line widths for $[MoO(SPh)_4]^-$ are due to the small **g** and **A** anisotropies for this anion; the slightly broader line widths of $[MoO(SePh)_4]^-$ will include a contribution from unresolved ^{77}Se ($I = 1/2$, 7.58 atom %) superhyperfine coupling. (ii) Greater **g** anisotropy broadens the lines in $[WO(XPh)_4]^-$. (iii) Greater **A** anisotropy (which contributes squared terms to the line-shape theory[32]) broadens the lines in $[MoOCl_4(MeCN)]^-$ and related species.

The narrow line widths of $[MoO(SPh)_4]^-$ encouraged examination of ^{17}O-enriched $[^{98}MoO(SPh)_4]^-$ in an attempt to detect ^{17}O ($I = 5/2$) superhyperfine coupling in the absence of the complications of ^{95,97}Mo hyperfine coupling (see Figure 3a). The room-temperature spectrum of $[^{98}MoO(SPh)_4]^-$ enriched with ^{17}O (24.9 atom %) in MeCN (Figure 6) shows well-developed coupling: $a(^{17}O) = 2.2 \times 10^{-4}$ cm^{-1}. The low-temperature glass spectrum (52.4 atom % ^{17}O) exhibits a slight broadening of the parallel component and a low-field shoulder on the perpendicular component. Accurate extraction of the anisotropic ^{17}O superhyperfine parameters was not possible. Independent reports[33,35] confirm the features reported here. No ^{17}O coupling was resolved for

(28) Bradbury, J. R.; Brunette, A. A.; McDonell, A. C.; Bond, A. M.; Wedd, A. G. *J. Am. Chem. Soc.*, following paper in this issue.
(29) Lane, R. W.; Ibers, J. A.; Frankel, R. B.; Papaefthymiou, G. C.; Holm, R. H. *J. Am. Chem. Soc.* **1977**, *99*, 84–98.
(30) (a) Garner, C. D.; Hillier, I. H.; Mabbs, F. E.; Taylor, C.; Guest, M. F. *J. Chem. Soc., Dalton Trans.* **1976**, 2258–2261. (b) Buluggia, E.; Vera, A. *J. Chem. Phys.* **1973**, *59*, 2886–2891.
(31) A detailed examination of the spin-relaxation mechanisms was hindered by the small temperature variation of the line widths of $[MoO(XPh)_4]^-$. For example, the line width of the $m_I = 1/2$ component at X-band frequency in $[^{95}MoO(SePh)_4]^-$ changed from 4.50 to 5.36 G over the range −6.6 to 57.5 °C. While the liquid range for MeCN is −45.7 to 81.6 °C, uncertainties in η and the reactivity of the species at temperatures above 50 °C frustrated effective extension of the temperature range. The experimentally observed line-width parameters at 300 K for $[^{95}MoO(SPh)_4]^-$ at X- and Q-band frequencies were, respectively: γ 0.040, 0.028 (0.033); β 0.247, 0.797 (0.798); $\alpha' + \alpha''$, 2.08, 4.40 (3.42) where the figures in parentheses are the Q-band parameters predicted theoretically from the X-band parameters; α'' 1.59 (0.21), 1.24 (0.26) where the figures in parentheses are the theoretical prediction assuming that the spin-rotational mechanism is the sole contributor to the line width. See text for further comment.
(32) (a) Atherton, N. M. "Electron Spin Resonance"; Wiley: New York, 1973; pp 327–358. (b) Wilson, R.; Kivelson, D. *J. Chem. Phys.* **1966**, *44*, 154–158, 4445–4452.
(33) Miller, K. F.; Stiefel, E. I., personal communication quoted in ref 34.

$[^{98}MoO(SePh)_4]^-$ and $[^{98}MoOCl_4(MeCN)]^-$ enriched with 24.9 atom % ^{17}O, presumably due to their intrinsically broader line widths (Table VI) and insufficient enrichment. The observation[34,35] of ^{17}O superhyperfine coupling of about (8–16) × 10^{-4} cm^{-1} in the molybdoenzymes xanthine oxidase, xanthine dehydrogenase, and sulfite oxidase in $^{17}OH_2$ demonstrates the presence of an exchangeable oxygen in the molybdenum coordination sphere. The magnitude of the coupling constants suggest that the exchangeable oxygen is an "in-plane" rather than an "axial" ligand.

Acknowledgment. Dr. J. R. Pilbrow and Dr. A. Edgar are thanked for their provision of computer simulation procedures and Q-band frequency measurements, respectively. A.G.W. thanks the Australian Research Grants Committee for financial support while G.R.H. acknowledges the award of a La Trobe University Postgraduate scholarship. K.S.M. acknowledges support from the Australian Research Grants Committee and a Monash University Special Research Grant. The assistance of Messrs. K. J. Berry and L. Mitchell with magnetic susceptibility measurements is gratefully acknowledged.

(34) Gutteridge, S.; Malthouse, J. P. G.; Bray, R. C. *J. Inorg. Biochem.* **1979**, *11*, 355–360.
(35) Cramer, S. P.; Johnson, J. L.; Rajagopalan, K. V.; Sorrell, T. M. *Biochem. Biophys. Res. Commun.* **1979**, *91*, 434–439.

Redox Properties of Thiolate Compounds of Oxomolybdenum(V) and Their Tungsten and Selenium Analogues

Julie R. Bradbury, Anthony F. Masters, Angus C. McDonell, Andrew A. Brunette, Alan M. Bond,*[1] and Anthony G. Wedd*

Contribution from the Department of Inorganic and Analytical Chemistry, La Trobe University, Bundoora, 3083, Australia, and the Division of Chemical and Physical Sciences, Deakin University, Waurn Ponds, 3217, Australia. *Received July 22, 1980*

Abstract: The rich electrochemistry of the mononuclear $[M^VO(XR)_4]^-$ and triply bridged binuclear $[M^V_2O_2(XR)_6Z]^{n-}$ anions (M = Mo, W; X = S, Se; R = Ph, *p*-tolyl, CH_2Ph; Z = uninegative (n = 1) or neutral (n = 0) ligand) is explored in MeCN and DMF at platinum and mercury electrodes over the temperature range +25 to −60 °C. Interconversion of the mononuclear and binuclear forms occurs via reduction and oxidation processes involving the metal and ligand centers. Stepwise reduction of the binuclear M^V_2 to $M^{IV,V}_2$ and M^{IV}_2 species is observed, and the reduced forms undergo chemical reactions which lead to the appearance of 1 molecule of $[M^{IV}O(XR)_4]^{2-}$/molecule of $[M^V_2O_2(XR)_6Z]^-$ reduced. In this way, the alkyl-substituted $[MoO(SCH_2Ph)_4]^{2-/-}$ ions can be generated at 25 °C. Chemically reversible, one-electron reduction of $[M^VO(XR)_4]^-$ is observed, while oxidation leads to the formation of $[M^V_2O_2(XR)_6Z]$ (Z = solvent) and RXXR via a process involving oxidative dissociation of ligand XR^-. For $[W^VO(XR)_4]^-$, the following one-electron couples are observed: $[W^{VI}O(XR)_4] + e^- = [W^VO(XR)_4]^-$ + $e^- = [W^{IV}O(XR)_4]^{2-}$. In view of the direct observation of $[W^{VI}O(XR)_4]$, an intramolecular redox step is apparently involved in the overall oxidation process described above. Wider implications of the ligand redox processes are discussed.

The molybdenum centers in the redox enzymes sulfite oxidase, xanthine oxidase and dehydrogenase, aldehyde oxidase, and nitrate reductase appear to cycle between the oxidation states VI, V, and IV during enzyme turnover[2] and, at least for sulfite oxidase and xanthine oxidase,[3] involve oxo and sulfur ligands. The present paper explores the rich redox chemistry of the mononuclear $[M^VO(XR)_4]^-$ (I) and triply bridged binuclear $[M^V_2O_2(XR)_6Z]^-$ (II) anions (M = Mo, W; X = S, Se; R = Ph, *p*-tolyl, CH_2Ph; Z = uninegative ligand) whose synthesis and electronic properties were described in the preceding paper.[4] The participation of thiolate ligand redox processes in the complex electrochemistry of these species is a significant observation. Preliminary redox aspects of the molybdenum–thiolate systems have been previously communicated.[5] The availability of the tungsten and selenium analogues permits a most detailed examination of the system.

Recent work[6–14] has considered the electrochemistry of various mono- and binuclear molybdenum complexes and, in particular, of compounds[11–14] of oxomolybdenum(V) containing multidentate thiolate ligands (including cysteine and its ethyl ester).

Experimental Section

All solution manipulations were carried out under purified argon or dinitrogen with use of standard techniques. Compounds were synthesized as described previously.[4,15,16]

Electrochemistry. The techniques employed were dc polarography at a dropping mercury electrode (dme), cyclic voltammetry (CV) at a

(1) Deakin University.
(2) Coughlan, M. P., Ed. "Molybdenum-Containing Enzymes"; Pergamon Press: Oxford, 1979.
(3) (a) Cramer, S. P.; Gray, H. B.; Rajagopalan, K. V. *J. Am. Chem. Soc.* **1979**, *101*, 2772–2774. (b) Tullius, T. D.; Kurtz, S. M.; Conradson, S. D.; Hodgson, K. O. *Ibid.* 2776–2779. (c) Bordas, J.; Bray, R. C.; Garner, C. D.; Gutteridge, S.; Hasnain, S. S. *J. Inorg. Biochem.* **1979**, *11*, 181–186.
(4) Hanson, G. R.; Brunette, A. A.; McDonell, A. C.; Murray, K. S.; Wedd, A. G. *J. Am. Chem. Soc.*, preceding paper in this issue.
(5) Bradbury, J. R.; Wedd, A. G.; Bond, A. M. *J. Chem. Soc., Chem. Commun.* **1979**, 1022–1025.
(6) Chalilpoyil, P.; Anson, F. C. *Inorg. Chem.* **1978**, *17*, 2418–2423.
(7) Lamache-Duhameaux, M. *J. Less-Common Met.* **1977**, *54*, 90.
(8) Wilshire, J. P.; Leon, L.; Bosserman, P.; Sawyer, D. T. *J. Am. Chem. Soc.* **1979**, *101*, 3379–3381.
(9) Hyde, J.; Venkatasubramanian, K.; Zubieta, J. *Inorg. Chem.* **1978**, *17*, 414–426.
(10) Schultz, F. A.; Ott, V. R.; Rolison, D. S.; Bravard, D. C.; McDonald, J. W.; Newton, W. E. *Inorg. Chem.* **1978**, *17*, 1758–1765.
(11) Ott, V. R.; Sweeter, D. S.; Schultz, F. A. *Inorg. Chem.* **1977**, *16*, 2538–2545.
(12) Howie, J. K.; Sawyer, D. T. *Inorg. Chem.* **1976**, *15*, 1892–1899.
(13) Bunzey, G.; Enemark, J. H.; Howie, J. K.; Sawyer, D. T. *J. Am. Chem. Soc.* **1977**, *99*, 4168–4170.
(14) Taylor, R. D.; Street, J. P.; Minelli, M.; Spence, J. T. *Inorg. Chem.* **1978**, *17*, 3207–3211.
(15) Boyd, I. W.; Dance, I. G.; Murray, K. S.; Wedd, A. G. *Aust. J. Chem.* **1978**, *31*, 279–284.
(16) Boyd, I. W.; Dance, I. G.; Landers, A. E.; Wedd, A. G. *Inorg. Chem.* **1979**, *18*, 1875–1885.

0002-7863/81/1503-1959$01.25/0